IMPACT ASSESSMENT OF UNCERTAINTY OF SPECTROSCOPIC PARAMETERS ON THE ACCURACY OF TRACE GASES ABUNDANCE

A thesis submitted to the School of Graduate Studies
Addis Ababa University

In partial Fulfilment of the Requirements for the
Degree of Master of Science in Physics

By

Samuel Takele

Addis Ababa, Ethiopia

July 2007

ADDIS ABABA UNIVERSITY
FACULTY OF SCIENCE
DEPARTMENT OF PHYSICS

The undersigned hereby certify that they have read and recommended to the Faculty of Science School of Graduate Studies for acceptance a thesis entitled "**IMPACT ASSESSMENT OF UNCERTAINTY OF SPECTROSCOPIC PARAMETERS ON THE ACCURACY OF TRACE GASES ABUNDANCE**" by **Samuel Takele** in partial fulfillment of the requirements for the degree of **Master of Science in Physics**.

Name	Signature
Dr. Gizaw Mengistu , Advisor	_____
Prof. Ashok. V. Gholap , Examiner	_____
Dr. Genene Tessema , Examiner	_____
Prof. Solomon Billilign, Examiner	_____

Dedicated to my family.

Acknowledgements

I would like to thank deeply my supervisor Dr. Gizaw Mengistu for his consistent help and constructive comment through out this MSc thesis work. I would like also to thank the ministry of education for paving a way for further study in Addiss Ababa University. And then I thank all my best friends and others who inspired me to be successful. Finally, I would like to extend my deep gratitude to my family for their support.

Addis Ababa, Ethiopia Samuel Takele

Abstract

We have studied sensitivity of the retrieved state vector (the atmospheric parameters) such as concentration (volume mixing ratio) profiles of targeted trace gases to uncertainty in spectroscopic parameters. Spectral line strength and pressure broadened half width of air are the spectroscopic parameters considered for this study. The atmospheric trace gases, for which the sensitives studies are performed, include source gases such H_2O, N_2O, CH_4 and SO_2, and stratospheric gases such as HNO_3 and O_3. The uncertainties of spectroscopic parameters considered ranges from 0.1% to 20% for spectral line strength and 0.1% to 3% for pressure broadened half width of air. The comparisons of difference of VMR of retrieved trace gases with and without perturbation of the spectroscopic parameters have shown different characteristics for different gases. The sensitivity is high at lower altitudes for source gases (H_2O, N_2O, CH_4) while the sensitivity for stratospheric gases (HNO_3 and O_3) is high at the altitude of peak VMR. In the case of SO_2, the impact is not noticeable, which is believed to be linked with undetectable level of SO_2 under normal atmospheric conditions.

Table of Contents

List of Figures

Introduction

Remote sensing techniques are an indirect method, which are currently widely used for deriving atmospheric parameters, such as temperature, pressure, and concentration of trace gases based on direct measurement of radiation emitted, absorbed and scattered by the atmosphere. In order to retrieve such atmospheric states, inversion(retrieval) algorithms such as SFIT2 software is employed [1]. Retrieval algorithms requires the radiative transfer equation for modelling the observed radiance in addition to measured radiance to derived atmospheric state parameters.

Radiative transfer theory (RT) employed in remote sensing application needs to describe the interaction between matter and electromagnetic radiation. There are two type of remote sensing techniques, these are passive remote sensing and active remote sensing. Passive remote sensing techniques make use of the interaction of natural radiation with the medium of interest, while active method employs artificial source of radiation such as lasers source [2]. The general remote sensing retrieval problem is non-linear and simplifying assumptions are made to reduce the problem to a linear one. Optimal estimation theory provides a method for estimating the state of the atmospheric on the basis of priori knowledge (usually a climatological profile) and the set of measurements made by the instrument. In general, the problem does not have a unique solution so an optimal solution from a number of possible solution is

selected.

Before considering the retrieval result, there are many components to consider when characterizing error sources in the retrieval process [3]. Spectroscopic parameters are non-retrieval atmospheric parameters, in which spectral line strength, line width, line position, partition function, and other parameters are included. These spectroscopic parameters are taken from the spectroscopic database such as high resolution atmospheric TRANsmission (HITRAN) database [4]. An accurate retrieval of quantities of interest requires accurate knowledge about the measurement and retrieval system. This includes knowledge of spectroscopic data. An uncertainty in spectroscopic parameters will lead to a systematic retrieval error [5]. Therefore, a thorough and careful investigation on the accuracy of the spectroscopic parameters and their impact on the retrieval are necessary.

Spectral line strength depends on both the properties of a single molecule and the population of the molecules in the upper and lower energy levels which in turn depends on the temperature of the environment [6]. Line width depends on temperature T, and on the colliding molecules (or the broadening gas), which can be separated into air broadening and self broadening parts [5]. The dependence of spectral line strength and line width on the atmospheric temperature is a clear evidence that accuracy by which we derive atmospheric state variables from remote sensing measurements. Therefore, in this work the two spectroscopic parameters are chosen to investigate how uncertainty of spectral line strength and line width parameters propagate to retrieved abundance of target trace gases in the atmosphere. In order to investigate the impact of these parameters, we have generated unperturbed and perturbed values of these

intended parameters from (HITRAN) database to use them in retrieval simulations. The retrieval simulations are performed based on optimal estimation method. The OEM allows one to perform an assessment of the model parameter error, such as the error coming from the intended parameter.

This thesis covers the spectroscopic parameters in chapter 1, radiative transfer and retrieval theory in chapter 2 and sensitivity studies with respect to uncertainty of spectroscopic parameter on retrieved state vector in Chapter 3. We present result and discussion of this research in chapter 4. Finally, we provide a conclusion of the thesis in chapter 5.

Chapter 1

Spectroscopic parameters

Spectroscopic parameters are non retrieval parameters which have an impact on the retrieval of atmospheric states (e.g. the concentration of trace gases). These spectroscopic parameters are spectral line strength, line width, line position, partition function, broadening parameters and others, which are recorded in the spectroscopic database such as HITRAN database.

1.1 Spectral line strength

Spectral line strength is a fundamental spectroscopic property of the absorbing species. The strength of the absorption is determined by the temperature dependent line strength, and the line shape function. The line shape function describes the temperature and pressure broadening mechanism of the fundamental line strength. The product of line strength and line shape function is the absorption cross section. The line strength depends on the properties of a single molecule and the population of the molecules in the upper and lower energy levels, which in turn depends on the temperature of the environment. If local thermodynamic equilibrium is assumed to

hold, Boltzmann distribution can be used to describe the number of molecules in a given state [6]. Under this circumstance, the line strength can be written as

$$S = \sigma(\frac{n_l - n_k}{n_{total}}) \tag{1.1.1}$$

where σ is absorption cross-section of a single species $\sigma = \frac{\hbar\omega}{c}B_{kl}$, n_k and n_l are population density of molecules in the upper and lower energy levels respectively. The relative populations are determined by Boltzmann's distribution (and hence as a function of temperature) according to $e^{-\frac{\Delta E}{KT}}$. The rate of absorption induced by the field is

$$W_{kl}(\omega) = \frac{\pi}{2\hbar^2}|E_o(\omega)|^2| < k|\epsilon.\mu|l > |^2\delta(\omega_{kl} - \omega) \tag{1.1.2}$$

The transition probabilities are greatest for the electric dipole transitions. But, for many pair of levels E_l and E_k, the quantity $< \phi_k| - er|\phi_l >$ vanishes which in turn leads to certain radiative selection rules. Radiative transition occurs only between certain pairs of levels. Transition dipole moment, for absorption is

$$\mu_{kl} =< \phi_k|\mu|\phi_l > \tag{1.1.3}$$

while for emission, it is given by

$$\mu_{lk} =< \phi_l|\mu|\phi_k > \tag{1.1.4}$$

where dipole moment is expressed as $\vec{\mu} = e\vec{r}$. Dipole moment (unit Coulomb meter) is simply a measure of how symmetric the charge distribution in the molecules. The more elongated the molecules, the larger the dipole moment, provided the molecule is somehow asymmetric. The strength of each spectral line is proportional to the square of the dipole moment. The presence of dipole moment is essential to absorb or emit radiation by molecules interacting with external electromagnetic field. Absorption

and emission that take place in the presence of an external field are called the induced absorption or emission. The rate is clearly dependent on the strength of the field. The variable that can be most easily measured is the intensity (energy flux through a unit area) which is the time averaged value of poynting vector,

$$S = \frac{c}{4\pi}(E \times B) \tag{1.1.5}$$

$$I =< S >= \frac{c}{4\pi} < E^2 >= \frac{C}{8\pi}E_o^2 \tag{1.1.6}$$

Another representation of the amplitude of the field is the energy density

$$U = \frac{1}{8\pi}E_o^2 \tag{1.1.7}$$

Substituting $eq(1.1.7)$ into $eq(1.1.2)$, then the following equation can be obtained

$$W_{kl}(\omega) = \frac{\pi}{2\hbar^2}U(\omega)| < k|\epsilon.\mu|l > |^2\delta(\omega_{kl} - \omega) \tag{1.1.8}$$

For an isotropic field

$$|E_o x| = |E_o y| = |E_o z| = \frac{1}{3}|E_o| \tag{1.1.9}$$

so that

$$W_{kl}(\omega) = \frac{4\pi^2}{3\hbar^2}U(\omega)| < k|\epsilon\mu|l > |^2\delta(\omega_{kl} - \omega) \tag{1.1.10}$$

Einstein coefficient B_{kl}, is written as

$$B_{kl} = \frac{4\pi^2}{3\hbar^2}|\mu_{kl}|^2 \tag{1.1.11}$$

For molecule in local thermodynamic equilibrium(LTE), all excitation temperature T of molecules, is the same, so that the population of each level is given by

$$n_l = \frac{n_{total}g_l}{Q(T)}e^{\frac{-E_l}{KT}} \tag{1.1.12}$$

and

$$n_k = \frac{n_{total} g_k}{Q(T)} e^{\frac{-E_k}{KT}} \tag{1.1.13}$$

where n_{total} - is the total column density of a species, $Q(T)$ is the total partition function. Substituting $eq(1.1.12)$ and $eq(1.1.13)$ into $eq(1.1.1)$, gives

$$S(T) = \frac{h\omega}{c} B_{kl} \left(\frac{g_l e^{\frac{-E_l}{KT}} - g_k e^{\frac{-E_k}{KT}}}{Q(T)}\right) \tag{1.1.14}$$

Substituting h and B_{kl} into equation(1.1.14), then gives

$$S(T) = \frac{8\pi^3 \omega}{3hc} |\mu_{kl}|^2 \left(\frac{g_l e^{-\frac{E_l}{KT}} - g_k e^{\frac{-E_k}{KT}}}{Q(T)}\right) \tag{1.1.15}$$

where h is the Planck constant, g_l and g_k are degeneracies of the lower and upper energy levels respectively, E_l and E_k are energies of lower and upper energy levels respectively. The lower state energy is obtained from the database, the upper state energy is calculated by $E_l = E_k + h\nu_{kl}$. The $e^{-\frac{E}{kT}}$ terms reflect the Boltzmann distribution of the energy level population, $|\mu_{kl}|$ is the magnitude of dipole moment of the molecule and $Q(T)$ is partition function [7]. Line strength at reference temperature is obtained from a spectroscopic database. The line strength at other temperature is obtained by an interpolation relation as

$$S(T) = S(T_o) \frac{Q(T_o)}{Q(T)} \left[\frac{exp[\frac{-E_l}{KT}] - exp[\frac{-E_k}{KT}]}{exp[\frac{-E_l}{KT_o}] - exp[\frac{-E_k}{KT_o}]}\right] \tag{1.1.16}$$

$$Q(T) = Q_{ele}(T) Q_{vib}(T) Q_{rot}(T) \tag{1.1.17}$$

where $Q_{ele}(T)$, $Q_{vib}(T)$, $Q_{rot}(T)$ are partition function of electronic, vibration, and rotational respectively.

1.2 Line width

Spectral line width is usually expressed in terms of full width at half maximum of the line (FWHM). Spectral lines can be broadened (that is the line width increased) by many physical mechanisms including natural, Doppler and collisional broadening. Natural broadening is the smallest of the three mechanisms and is a direct result of the Heisenberg uncertainty principle. In the atmosphere both Doppler and collisional broadening are important where the lineshape may involve a combination of the two effects [8]. One example is the Voigt line shape. In the following section, we discuss how line width parameters would be changed due to different physical mechanisms.

1.2.1 Doppler broadening

The cause of line broadening comes from the thermal motion of the molecules leading to doppler shift of the central frequency. In thermal equilibrium, the velocity of molecules follows a gaussian distribution and the doppler line shape function can be described as

$$F_D(\nu, \nu_o) = (\sqrt{\pi}\gamma_D)^{-1} e^{-|\frac{\nu-\nu_o}{\gamma_D}|^2}, \tag{1.2.1}$$

and

$$\gamma_D = \frac{\nu_o}{c}\sqrt{\frac{2RT}{M}} \tag{1.2.2}$$

where γ_D is the Doppler induced width of the line, M is the molecular weight in atomic mass unit, ν_o is central line frequency, c is speed of light and R is the universal gas constant. This line broadening mechanism gets stronger with increasing frequency and is not related to pressure.

1.2.2 Pressure broadening

The collisions between molecules in the atmosphere results in the shortening of the lifetime of the states involved in the transition and therefore the corresponding line will be broadened. The related line broadening function will have a shape described by the Lorenz function:

$$F_L(\nu, \nu_o) = \frac{1}{\pi} \frac{\gamma_p}{(\nu - \nu_o)^2 + \gamma_p^2} \tag{1.2.3}$$

where γ_p is the pressure induced width of the line. The full width at half maximum (FWHM) of the line is $2\gamma_p$. This value changes with pressure and temperature according to

$$\gamma_p = \gamma_o (\frac{P}{P_o})(\frac{T_o}{T})^x \tag{1.2.4}$$

where γ_o is the line pressure broadening width at reference pressure, P_o and temperature, T_o and x is an empirical parameter for the temperature dependency generally varying between 0.5 and 1. As this phenomenon is directly proportional to the pressure and therefore the altitude, the width of the line induced by pressure broadening can be used to retrieve the height information on concentration of trace gases.

1.2.3 Voigt line shape

When doppler and pressure broadening mechanisms have the same magnitude, the resulting line shape is a convolution of the Doppler and the Lorentz line shape called the Voigt line shape.

$$F_{voigt}(\nu, \nu_o) = \int_{-\infty}^{\infty} F_L(\nu - \nu', \nu_o) F_D(\nu, \nu_o) d\nu \tag{1.2.5}$$

In the mid infrared, spectral line width due to Doppler and pressure broadening become equal at around 30 km. A radiative transfer model has to consider the spectral line shape of line source from surrounding altitudes to model the most accurate representation of the true atmosphere. The Voigt line shape adequately describes the combined behavior of both mechanisms in the atmospheric applications. This provides a convolution of the doppler and pressure-broadened(Lorentz) line shapes:

$$k(\nu) = \frac{S}{\alpha_D \sqrt{\pi}} \frac{y}{\pi} \int_{-\infty}^{\infty} \frac{e^{-t^2}}{y^2 + (x-t)} dt \tag{1.2.6}$$

where $k(\nu)$ is the absorption coefficient at some wave number ν. S is the line intensity at some reference coefficient line center, ν_o and t is the duration of emission. Also, x and y are defined as

$$x = \frac{\alpha_l}{\alpha_D} \tag{1.2.7}$$

$$y = \frac{\nu - \nu_o}{\alpha_D} \tag{1.2.8}$$

where α_L and α_D are the lorentz and doppler half widths respectively [9].

1.3 Line position

Line position is the center of the absorption or emission line, and with the most recent techniques it can be determined with very good accuracy ($10^{-10} Hz$ or better). It is determined by

$$\nu = \frac{E_{upper} - E_{lower}}{h} \tag{1.3.1}$$

with h being Planck's constant. With appropriate quantum theoretical models one can reproduce the line positions within experimental accuracy, except for difficult molecules (eg. with interacting states or large-amplitude motions). Note that the

knowledge of the lower states energy is important to predict the spectral intensities at different temperature [10].

1.4 Partition function

In statistical mechanics, the partition function is an important quantity that encodes the statistical properties of a system in thermodynamic equilibrium. It is a function of temperature and other parameter, such as the volume enclosing a gas. Most thermodynamic variable of the system such as the total variable of the system, total energy, free energy, entropy and pressure can be expressed in terms of partition function or its derivatives. Molecular energy levels arise from molecular translation (motion through space), rotation, vibration, and electronic excitation. For atmospheric applications we focus on the infrared region which involves mostly vibrational and rotational transition. This information constitutes the spectroscopy of a molecule of interest and can be obtained experimentally or from calculation. Molecular energy levels E_j are used to compute the molecular partition function, usually denoted by the symbol q, as

$$q = \sum_j e^{-\beta E_j} \tag{1.4.1}$$

where $\beta = \frac{1}{k_B T}$, k_B is Boltzmann's constant, E_j energy of level j. For degenerate states the partition function becomes

$$q = \sum_j g_j e^{-\beta E_j} \tag{1.4.2}$$

where g_j is degeneracy factor. Degeneracy is the number of levels of equal energy in which a molecule may lie. One typically chooses the lowest energy levels to be the zero of energy, so that no levels lie at negative energies. So there are different types

of partition function due to various internal molecular energy levels (states) which change in accordance with the amount of energy that imposed on the molecules. For the sake of completeness, we describe briefly all the partition functions in the following section.

1.4.1 Translation partition function

The translation partition function is the sum overall available translation energy states. Since this is continuous, we use an integral for the sum in eqn(1.4.1):

$$q_{tra} = \int_0^\infty \omega(\epsilon) e^{-\beta\epsilon} d\epsilon \tag{1.4.3}$$

The integral represents the number of energy states between ϵ and $\epsilon + d\epsilon$ multiplied by the effective degeneracy of each state. We can use the particle in a 3-D infinite well to understand the degeneracy $\omega(\epsilon)$. The energy levels of a particle in a 3-D infinite well are

$$\epsilon_{n_x,n_y,n_z} = \frac{\hbar}{8ma^2}(n_x^2 + n_y^2 + n_z^2) \tag{1.4.4}$$

The degeneracy is just the number of ways that R can be written as the sum of three positive integers. Now consider a portion of sphere where $n_x > 0$, $n_y > 0$, and $n_z > 0$

$$n_x^2 + n_y^2 + n_z^2 = R^2 = \frac{8ma^2\epsilon}{\hbar} \tag{1.4.5}$$

where m is the mass of particle, and a is radius. From this, we can examine the number of states with a given energy.

The number of states with energy $\leq \epsilon$ is

$$\Phi(\epsilon) = \frac{1}{8}(\frac{4\pi R^3}{3}) = \frac{\pi}{6}(\frac{8ma^2\epsilon}{\hbar^2})^{\frac{3}{2}} \tag{1.4.6}$$

Going one step further we can look at the number of states between ϵ and $\epsilon + \Delta\epsilon$ (i.e. the degeneracy):

$$\omega(\epsilon, \Delta\epsilon) = \Phi(\epsilon + \Delta\epsilon) - \Phi(\epsilon) \tag{1.4.7}$$

$$= \frac{\pi}{6}(\frac{8ma^2}{\hbar^2})^{\frac{3}{2}}[(\epsilon + \Delta\epsilon)^{\frac{3}{2}} - \epsilon^{\frac{3}{2}}] \tag{1.4.8}$$

$$= \frac{\pi}{6}(\frac{8ma^2}{\hbar^2})^{\frac{3}{2}}[\epsilon^{\frac{3}{2}} + \frac{3}{2}\epsilon^{\frac{3}{2}}\Delta\epsilon - \epsilon^{\frac{3}{2}}....] \tag{1.4.9}$$

$$\omega(\epsilon, \Delta\epsilon) = \frac{\pi}{4}(\frac{8ma^2}{\hbar^2})^{\frac{3}{2}}\epsilon^{\frac{3}{2}}\Delta\epsilon + \textit{higher order} \tag{1.4.10}$$

which leads to final expression for degeneracy

$$\omega(\epsilon)d\epsilon = \frac{\pi}{4}(\frac{8ma^2}{\hbar^2})^{\frac{3}{2}}\epsilon^{\frac{1}{2}}d\epsilon \tag{1.4.11}$$

Substituting eqn(1.4.11)into the original integral, we obtain an expression for the translation partition function

$$q_{tran} = \int_0^\infty \frac{\pi}{4}(\frac{8ma^2}{\hbar^2})^{\frac{3}{2}}e^{-\frac{\epsilon}{KT}}d\epsilon \tag{1.4.12}$$

$$q_{tran} = (\frac{2\pi mKT}{\hbar^2})^{\frac{3}{2}}V \tag{1.4.13}$$

1.4.2 Vibrational partition function

Vibrational energy levels are discrete so that the vibrational partition function is just the sum over all states. To derive the partition function, we take the energy levels for simple harmonic oscillators. A molecule that contains N atoms has 3N-6 vibrational frequencies (3N-5 for linear molecule). The quantized form of energy for simple harmonic oscillator is written as

$$\varepsilon_n = (n + \frac{1}{2})h\nu \tag{1.4.14}$$

where n= 1,2,... The total vibrational energy is then

$$\varepsilon_{vib} = \sum_{n=1}^{\infty}(n + \frac{1}{2})h\nu \tag{1.4.15}$$

From the definition of a partition function, we can write the total vibrational partition function as

$$q_{vib} = \sum e^{\beta\epsilon} = e^{\frac{-\beta h\nu}{2}} \sum_{n} e^{-\beta n h\nu} \tag{1.4.16}$$

$$q_{vib} = \frac{e^{\frac{-\beta h\nu}{2}}}{1 - e^{-\beta h\nu}} \tag{1.4.17}$$

In general, for a molecule the vibrational partition function is just a product of the partition function for each vibrational mode

$$q_{vib} = \prod_{i=1}^{\infty} \frac{e^{\frac{-\beta h\nu}{2}}}{1 - e^{-\beta h\nu}} \tag{1.4.18}$$

1.4.3 Rotational partition function

The derivation of a rotational partition function is analogous to that for the vibrational partition function. The only difference is that the rotational energy levels are dependent on the geometry of the molecule. Hence, there are different rotational partition functions for different geometrical classes of molecules. As an example, the derivation is included here for a linear molecule. For linear molecule, we can take the energy from the energy levels for a rigid rotor:

$$E_J = \frac{J(J+1)h^2}{8\pi^2 I} \tag{1.4.19}$$

where J is the rotational quantum number ($J = 0, 1, 2, ...$) and I the moment of inertia given by:

$$I = \sum_{l=1}^{\infty} m_l d_l^2 \tag{1.4.20}$$

Therefore, the rotational partition function q_{rot} is

$$q_{rot} = \frac{1}{\sigma}\sum_{J=0}^{\infty}(2J+1)e^{\frac{-\theta_{rot}J(J+1)}{T}} \tag{1.4.21}$$

where $\theta_{rot} = \frac{\hbar^2}{2IK}$, σ - symmetry number. σ takes a value of $\sigma = 1$ for unsymmetrical molecules $\sigma = 2$ for symmetric molecules. For $\theta_{rot} << T$,

$$q_{rot} \simeq \frac{1}{\sigma}\int_{J=0}^{\infty} J(J+1)e^{\frac{-\theta_{rot}J(J+1)}{T}}dJ \tag{1.4.22}$$

$$= \frac{1}{\sigma}\int_{J}^{\infty} e^{\frac{-\theta_{rot}}{T}}dy \tag{1.4.23}$$

$$= \frac{1}{\sigma}[\frac{-T}{\theta_{rot}}e^{\frac{-\theta_{rot}}{T}}]_0^{\infty} = \frac{1}{\sigma}[\frac{T}{\theta_{rot}}] \tag{1.4.24}$$

$$q_{rot} = \frac{8\pi^2 IKT}{\sigma h^2} \tag{1.4.25}$$

where y=J(J+1)

1.4.4 Electronic partition function

The excited electronic states of most molecules are so much higher in energy than the ground electronic state (relative to K_BT) the approximation of q_{ele} is usually a good one though there are some notable exceptions [11]. Thus, the partition function is expressed as

$$q_{ele} = \sum_i \omega_{ei}e^{-\beta\epsilon_i} \tag{1.4.26}$$

Chapter 2

Radiative transfer and Retrieval theory

2.1 Radiative transfer equation

Radiative transfer is the most fundamental concept in the study of atmospheric radiation. Indeed, remote sensing observations are only possible due to the transfer of radiation through the atmosphere to the instrument. The radiation arriving at an observing instrument is the sum of radiation entering the atmosphere in the field of view of the instrument and that emitted or scattered by trace gases such as H_2O, O_3, aerosol or by cloud into the beam of radiation. The intensity, or radiance, of the beam of energy originating from a point can be attenuated within a differential thickness ds by

$$dI_\nu = -e_\nu n_a I_\nu ds \tag{2.1.1}$$

where e_ν is the molecular extinction coefficient constant that characterize the radiation matter interaction (including both absorption and scattering), and n_a is the number density of absorbing atoms or molecules. In a path ds, the absorbing or scattering molecules may also contribute to the incident radiation through emission.

The increase in radiance travelling through the path ds is then given by

$$dI_\nu = j_\nu n_a ds \tag{2.1.2}$$

where j_ν is the emission coefficient constant, which characterizes the emission properties of the molecules in the path. Assuming that the atmospheric layer is in local thermodynamic equilibrium (LTE) at a given temperature T, Kirchhoff's law can be used to relate states that the emission and absorption coefficients, j_ν and e_ν by

$$\frac{j_\nu}{e_\nu} = f_\nu(T) \tag{2.1.3}$$

where J_ν source function. Therefore, equation(2.1.2)can be rewritten

$$dI_\nu = e_\nu n_a J_\nu ds \tag{2.1.4}$$

Extinction and emission must combine to give a net change in radiance. This change is expressed as

$$\frac{dI(P,s)}{ds} = -e_\nu n_a [I_\nu(P,s) - J_\nu(P,s)] \tag{2.1.5}$$

where $I_\nu(P,s)$ defines the radiance at a point P in an arbitrary direction s. This is Schwarzchild's radiative transfer equation. In the absorption process, a photon excites the matter into one of its internal energy modes, while in emission, the reverse process, an excited state is deactivated by emitting a photon. Absorption is often followed by energy transfer of the excited internal energy mode to translational energy in a subsequent matter-matter interaction. Energy of a photon may be re-emitted, or simply transferred to some other internal state of the molecule or one of its collision partners. The effects of simple scattering are usually negligible in infrared atmospheric radiative transfer, so ignoring simple scattering implies that the extinction coefficient

is the same as the absorption coefficient:

$$e_\nu = k_\nu \tag{2.1.6}$$

and so the emission term is given by

$$e_\nu n_a J_\nu = k_\nu n_a J_\nu \tag{2.1.7}$$

where J_ν exclude "simple scattering ". Both absorption and emission are assumed to be isotropic (i.e. there is no dependence of k_ν and J_ν on the angular distribution of photons).

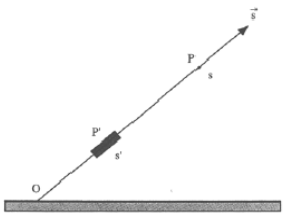

Figure 2.1: Optical depth

To apply the radiative transfer equation to remote sensing problems, let us consider the optical depth of radiation from source to the instrument as shown in Fig 2.1. The optical thickness τ_ν describes the total optical path length in atmospheric medium, between two points s' and s along the direction **s** defined by:

$$\tau_\nu(s', s) = \int_{s'}^{s} k_\nu(s")n_a(s")ds" \tag{2.1.8}$$

The radiative transfer equation at the point P' at a distance s can now be written as

$$\frac{dI_\nu(s',s)}{d\tau_\nu} = [I_\nu(s',s) - J_\nu(s',s)] \tag{2.1.9}$$

where τ_ν is defined as a positive quantity as $s > s'$. As equation is a linear first-order differential equation with constant coefficient, the necessary integrating factor is $exp(-\tau_\nu)$. Multiplying equation(2.1.9) by this factor gives

$$\frac{d[I_\nu(s',s)exp(-\tau_\nu)]}{d\tau_\nu} = -exp(-\tau_\nu)J_\nu(s',s) \tag{2.1.10}$$

After integration using $\tau_\nu = 0$, at the origin s_o:

$$I_\nu(s',s) = I_\nu(s_o,s)exp[-\tau(s_o,s)] + \int_o^{\tau(s_o,s)} J_\nu(s',s)exp[-\tau(s',s)]d\tau_\nu \tag{2.1.11}$$

Equation 2.1.11 solves the radiative transfer problem if the source function $J_\nu(P',s)$ at a point P' and direction $\mathbf{s}$ is known. Under local thermodynamic conditions the source function is given by the Planck function, $B_\nu(T)$. The Planck function is given by

$$B_\nu(T) = \frac{2h\nu^3}{c^2}\frac{1}{[exp(\frac{h\nu}{k_BT}) - 1]} \tag{2.1.12}$$

where h is Planck's constant, and k_B the Boltzmann constant. At a given frequency, the source function depends only on temperature T, if the gas is in thermodynamic equilibrium. Different gas properties emitting and absorbing radiation at frequency ν are contained in their absorption or emission coefficient, k_B. One can also use transmission model equally well to describe the measurement $e^{-\tau}$ is the total transmission between the points corresponding to optical path $\tau = 0$, the top of atmosphere, and $\tau = \tau$, at the site of the instrument. The radiative transfer model in terms of total transmission has the form

$$I_\nu(t) = B_\nu(T_s)t \tag{2.1.13}$$

We then note that attenuation of radiation between arbitrary atmospheric layers bounded by s' and s is described as

$$I_\nu(t) = B_\nu(T_s) \int_{s'}^{s} \frac{\partial t}{\partial s"} ds" \tag{2.1.14}$$

where now t is the total transmission after being attenuated by gases within layers bounded by $s"$ and $s" + ds"$. This is the general model for which explicit functional form of τ is not given, however, recalling the definition of optical thickness, the transmission can expressed as a function of s'.

$$t_\nu(s', s) = exp(-\int_{s'}^{s} k_\nu(s")n_a(s")ds") \tag{2.1.15}$$

As there are many absorber along the optical path, the absorption cross-section is weighted and given by

$$k_\nu(s') = \sum_{m=1}^{M} k_{\nu(m)}(s')y_m(s') \tag{2.1.16}$$

where $y_m(s')$ and $k_{\nu(m)}(s')$ stand, respectively, for volume mixing ratio (vmr) and absorption cross section of the species m of the total number M of different molecular species that absorb in the spectral region under consideration. Then, by substituting equation(2.1.16) into equation(2.1.11), we can obtain the equation as follows

$$I_\nu(s', s) = I_\nu(s_o, s)exp[-\int_{s_o}^{s} \sum_{m=1}^{M} k_{\nu(m)}(s')y_m(s')\rho(s')ds'] \tag{2.1.17}$$

Dividing the above equation by $I_\nu(s_o, s)$, gives

$$\frac{I_\nu(s', s)}{I_\nu(s_o, s)} = exp[-\int_{s_o}^{s} \sum_{m=1}^{M} k_{\nu(m)}(s')y_m(s')\rho(s')ds'] \tag{2.1.18}$$

Further more, as the molecular species m may have several transitions which have different temperature and pressure dependence, the absorption cross-section of one molecular species m as a function of temperature and pressure is given by the following

sum over all lines of the species (more details on the above discussion can be found [12, 13, 14, 15].

$$k_{\nu(m)}(T,P) = \sum_{l=1}^{lines} S_{m,l}(T) g_{m,l}(\nu - \nu_{m,l}, T, P) \tag{2.1.19}$$

where $g_{m,l}(\nu - \nu_{m,l}, T, P)$ is line shape function and $S_{m,l}(T)$ is spectral line strength described briefly in section (1.2).

2.2 Retrieval theory

The retrieval of atmospheric parameters from remote sensing data requires accurate calculations that determine the received radiation for specific atmospheric conditions, since the sensor measures complicated functions of the quantities of interest. These measurements do not give the actual state of the atmosphere with independent errors, but only the best estimate derivable from the measurements and prior knowledge about the state of the atmosphere. Thus, the intensity and spectral distribution can be calculated given the profiles of the constituents in the atmosphere and relationship between altitude, pressure and temperature.

2.2.1 Optimal estimation Method

The Optimal estimation method describes the relationship between the remote measurements and the true atmospheric state, with an extensive analysis of errors involved. It is a special case of model fitting that minimizes the difference between model prediction and measurement, by adjusting fit parameters. The mathematical representation of quantities measured in any remote sensing is given by [16]:

$$Y = F(x,b) + \epsilon_y \tag{2.2.1}$$

where y is the vector of the measured intensities for certain frequencies, x the vector of the intended constituent profiles, b a set of model parameters comprising quantities that influence the measurements and are known to some accuracy, e.g. the relationship between altitude, pressure and temperature, ϵ_y the experimental error contribution and F is the forward model which provides a physical description of the measurement process and a numerical process provides simulation of the radiative transfer in the experiment. The purpose of the forward model is three-fold: namely, to study the information potentially available in the measurement, to assist in the design of the instrument and to form part of the data retrieval system. The derivation of the desired atmospheric parameters from the instrument signals is an inversion process, and an accurate forward model is necessary for a successful retrieval [17, 18]. However, equation(2.2.1) can not be directly implemented in remote sensing, since a set of constituent profiles has to be retrieved from a measured intensity distribution. Thus, the inversion of the radiative transfer equation is required to implement it for remote sensing applications as shown in equation(2.2.2). This requires a numerical approach, as there is no analytical solution for the equation (2.2.2). An inverse (or retrieval) method R has to be applied to the measurement vector in order to retrieve an optimal estimate $\hat{x}$ of the state vector x, i.e.,

$$\hat{x} = R(y) \tag{2.2.2}$$

By using a χ^2_ϵ cost function, the numerical solution minimizes the difference between a measurement y and a model calculation F(x,b). The cost function is given by

$$\chi^2_\epsilon = [y - F(x,b)]^T S_\epsilon^{-1} [y - F(x,b)] \tag{2.2.3}$$

where S_ϵ is the measurement covariance matrix. S_ϵ gives the errors and their correlation with the measurement vector y. However, it is necessary to use additional apriori information about the state of the atmosphere in order to constrain the retrieval. This can be a climatology derived from set of independent measurements of the atmospheric constituents to be retrieved. It is important because several atmospheric states x may exist that satisfy equation(2.2.2) for a measured radiation distribution y, leading to finite measurements for continuous unknowns. This makes the inversion ill-conditioned. Similarly, noise amplification can be prevented by constraining the retrieval since small errors in the measured quantity y leads to large errors in the retrieved quantity x [19]. The additional information leads to a second χ^2 term as given below

$$\chi_a^2 = [x - x_a]^T s_a^{-1} [x - x_a] \tag{2.2.4}$$

where x_a is the vector containing the apriori information and S_a is the apriori covariance matrix taken from the climatology. Finally, the total cost function $\chi^2 = \chi_\epsilon^2 + \chi_a^2$ is minimized, i.e.

$$\chi^2 = [y - F(x)]^T S_\epsilon^{-1} [y - F(x)] + [x - x_a] S_a^{-1} [x - x_a] \tag{2.2.5}$$

The minimum of the cost function is found depending on the non-linearity of the forward model. For an optically thin atmosphere, i.e. atmosphere whose optical thickness approximately equals to zero, the forward model in equation (2.2.1) can be replaced with a matrix so that the inversion can be done with simple matrix algebra. This is totally linear case. But since such assumption is not applicable in the context of this work. For a forward model that is strongly non-linear, sophisticated iteration schemes like the Levenberg-Marquardt method can be used [16, 20].

2.2.2 Iterating and convergence

The optimal estimation retrieval approach finds the most probable solution consistent with both the measurements and the a priori knowledge. In the non-linear case, this requires the solving of a complex equation relating all of the measurements, a priori knowledge, the forward model parameters and other inputs to the retrieval. The maximum a posteriori (MAP) approach can be used to solve non-linear problems. Defining x and y as vector random variables. A vector random variable is described by its probability density function (pdf). A vector x has a pdf written as P(x) and y has a pdf P(y). Once the measurement y, is made the pdf of x is then $P(x|y)$. From Bayes theorem

$$P(x|y) = \frac{P(y|x)P(x)}{P(y)} \tag{2.2.6}$$

This method requires the minimization of a cost function which, for gaussian errors and using a Bayesian approach, is:

$$-2lnP(x|y) = [y - F(\hat{x})]^T S_y^{-1}[y - F(\hat{x})] + [\hat{x} - x_a]^T S_a^{-1}[\hat{x} - x_a] + constant \tag{2.2.7}$$

Finding the zero gradient of the cost function, or in other words the minimum yields [21]

$$\nabla_x -2ln(x|y) = [\nabla_x F(\hat{x})]^T S_y^{-1}[y - F(\hat{x})] + S_a^{-1}[\hat{x} - x_a] = 0 \tag{2.2.8}$$

As $\nabla_x F(x) = K(x)$ the equation to be solved is

$$-K^T S_y^{-1}[y - F(\hat{x})] + S_a^{-1}[\hat{x} - x_a] = 0 \tag{2.2.9}$$

If the forward model is linear, i.e., $F(\hat{x}) = K\hat{x}$, then the solution for $\hat{x}$ follows:

$$\hat{x} = x_a + (K^T S_y^{-1} K + S_a^{-1})^{-1} K S_y^{-1}(y - Kx_a) \tag{2.2.10}$$

with the covariance given by:

$$\hat{S} = (K^T S_y^{-1} K + S_a^{-1})^{-1} \tag{2.2.11}$$

and its averaging kernel matrix is defined as:

$$A = (K^T S_y^{-1} K + S_a^{-1})^{-1} K^T S_y^{-1} K \tag{2.2.12}$$

Optimal estimation method allow the characterization of the retrievals, ie., the vertical resolution of the retrieval, its sensitivity to the priori information and the degree of freedom. This is obtained by considering that the retrieve state vector $\hat{x}$ is related to the true state vector x by

$$\hat{x} = x_a + A(x - x_a) + \textit{error terms}, \tag{2.2.13}$$

The retrieved parameters are weighed means of the true and a priori state vector parameters. The weight associated with the true state vector parameters is given by the average kernel matrix A which would be the identity matrix in an ideal case where the retrieval would reproduce the truth. The actual average kernel matrix depends on several parameters including the solar zenith angle, the spectral resolution and signal-noise-ratio, the choice of retrieval microwindow and the priori covariance matrix S_a [13].

Non-linear problems are best solved by some form of iteration technique, for example by linearizing the problem and using a linear optimal method solution. Another class of moderately nonlinear problems require other methods to find the solution efficiently but are sufficiently linear in the neighborhood of the solution for linearization to be used in the error analysis. These problems require a regularization factor in

the iteration scheme; a common variation of Newtonian iteration and used in the retrieval schemes is the Levenburg-Marquardt iteration technique [17]. The convergence criteria for retrieval is performed through an iterative procedure aimed at reaching the minimum of χ. The convergence criteria determine when the iterative procedure stops (see for detail [23]).

If the problem is not too non-linear then Newtonian iteration can be used to find the best estimate of the state $\hat{x}$. Newton's method for finding the zero of a scalar function f(x) of one variable is

$$x_{n+i} = x_i - (\frac{df(x_i)}{dx})^{-1} f(x_i) \tag{2.2.14}$$

The version for a vector-valued function of a vector, g(x), is

$$x_{n+i} = x_i - (\nabla_x g(x_i))^{-1} g(x_i) \tag{2.2.15}$$

where the inverse is a matrix inverse. Applying g(x) to the maximum a posteriori problem

$$g(x) = K^T S_y^{-1}[y - F(\hat{x})] + S_a^{-1}[\hat{x} - x_a] \tag{2.2.16}$$

$$\nabla_x g = -\nabla_x K^T S_y^{-1}[y - F(\hat{x})] + K^T S_y^{-1} K + S_a^{-1} \tag{2.2.17}$$

$\nabla_x K^T$ is usually small compared to the other terms, so ignoring this terms the iteration becomes

$$x_{i+1} = x_i - (S_a^{-1} + K_i^T S_y^{-1} K_i)^{-1}(-K_i^T S_y^{-1}[y - F(x)] + S_a^{-1}[x_i - x_a]) \tag{2.2.18}$$

By expressing x_{i+1} as a departure from rather x_a then equation(2.2.18) can be rearranged in the form:

$$x_{i+1} = x_a + (S_a^{-1} + K_i^T S_y^{-1} K_i)^{-1} + (K_i^T S_y^{-1}[y - F(x)] + K_i[x_i - x_a]) \tag{2.2.19}$$

It is usually common to start the iteration at $x_o = x_a$.

The levenberg-Marquardt Iteration technique is similar to Gauss-Newton iteration but with the addition of an extra constant term, γ, which aids convergence

$$x_{i+1} = x_i - (S_a^{-1} + K_i^T S_y^{-1} K_i + \gamma D)^{-1}(-KS[y - F(x_i)] + S_a^{-1}[x_i - x_a]) \quad (2.2.20)$$

where D is a necessary diagonal scaling matrix; the simplest choice is to set it equal to S_a^{-1}. The value of γ determines the step size used at each iteration. If the value obtained from the iteration reduces the error, the new estimate, x_{i+1}, is accepted and γ is divided by ten. If the error increases on x_{i+1}, however, then γ is multiplied by ten and equation(2.2.20) is solved again until an increment is obtained that reduces the error. There are many other methods that can be used for iterating towards a solution but they are mostly variations of the two approaches described in these sections. In general the other schemes require some "tweaking" of a parameter at each iteration step which in turn determines the step size but can also determine the direction in which the solution moves [12].

2.2.3 The relationship between spectroscopic parameters and state vectors

We linearized the forward model $y = F(x, b)$ around the apriori estimate x_a taken as first guess:

$$y = F(x_a, b) + K_x(x - x_a) + O((x - x_a)^2) \quad (2.2.21)$$

Similarly, we linearize forward model around b_a which is the best estimate of spectroscopic parameters.

$$y = F(x, b_a) + K_b(b - b_a) + O((b - b_a)^2) \tag{2.2.22}$$

The Jacobian matrix is a linearization of the forward model that enables application of matrix algebra to the inverse problem. It represents the sensitivity of the observation variables y to the state variables x, assembled in matrix form:

$$K_x = \nabla_x F = \frac{\partial y}{\partial x} \tag{2.2.23}$$

If the forward model is linear, then K does not depend on x and fully describes the forward model for the purpose of the inversion. If the forward model is not linear, then K is a function of x and represents a linearization of the forward model around x. It needs to be calculated initially for the a priori value x_a, representing the initial guess for x, and then re-calculated as needed for updated values of x during iterative convergence to the solution. Depending on the degree of non-linearity, K may not need to be re-calculated at each iteration [24]. From equation(2.2.22), the term K_b represents the sensitivity of the observation variables y to the spectroscopic parameters b, assembled in matrix form:

$$K_b = \nabla_b F = \frac{\partial y}{\partial b} \tag{2.2.24}$$

In order to obtain the change of forward model simulation (δF) and change of concentration (δx) of the species due to uncertainty of spectroscopic parameters (b) we use

$$\delta F = F(x, b + \delta b) - F(x, b) \tag{2.2.25}$$

$$\delta x = x(b + \delta b) - x(b) \tag{2.2.26}$$

Based on the above equations, we can show the numerical relationship of δx with δb as well as with δF with δb. In this work, the intensity ratio (referring equation (2.2.19) is maintained constant in the retrieval simulation since it is a measured value, so that we can easily investigate the relationship of the spectroscopic parameters with the retrieved state vector.

2.3 Retrieval scheme

The retrieval procedure used in this work is SFIT2 software algorithm, which incorporates Rodgers' formulation of the Optimal Estimation Method (OEM) with an iterative Newton scheme. SFIT2 was developed at NASA' s Langley Research Center (LaRC) and the National Institute of Water and Atmosphere (NIWA). The main element of the software is the forward model that creates a synthetic spectrum from a simulated atmosphere. It then fits the measured spectrum and the synthetic spectrum using optimal estimation. The parameters used in the retrieval procedure, including simultaneous retrievals of several wavelength region, interfering molecules, and diagonal values of the measurement and a priori profile error covariance matrices S_a and S_ϵ. This makes it possible to combine several individual microwindows, combining saturated lines with good tropospheric sensitivity, with weaker lines yielding stratospheric sensitivity [25].

Chapter 3

Sensitivity studies with respect to uncertainty of spectroscopic parameter on retrieved state vector

3.1 Error analysis

Error analysis is meant the sensitivity of the retrieval to all sources of error in the transfer function. The total error of the retrieval consists of random and systematic error components, depending on whether they are identical between separate measurements, or vary randomly between them. In this analysis, the systematic error of the retrieval is calculated. Other terms that are related to the exactness of measurement with one another are precision (the variability between repeated measurements of the same state) and accuracy (the total difference between the measurement and the truth). From practical measurements the difference between the two can be indistinct, depending on the variability of the error over time. An error which is systematic on one scale may be totally random on another. From a priori data, Jacobian, averaging kernel matrix and covariance matrices, it is possible to compute some indicators giving us information about the characteristics such as expected error (corresponding to the uncertainty on the retrieved value), vertical resolution or measurement response of the retrieval process [12, 25, 26]. There are four major sources of error in

the retrieval such as retrieval noise, forward model parameter error, forward model error, and smoothing error which are discussed briefly in the following section but particularly the emphasis is given for forward model parameters error in this studies. In order to perform a basic error analysis, the Jacobian of the measurement is important. The forward model F is linearized about $x = x_a$ and $b = b_a$ which are expressed in eq(2.2.23) and eq(2.2.24) respectively while the retrieval method R is linearized about $y = F(x_a, b_a)$,

$$G_y = \frac{\partial R(y,b)}{\partial y}|_{y=F(x,b)} \tag{3.1.1}$$

$$x - x_b = G_y\epsilon + G_yK_b(b - b_a) + G_y\Delta f(x, b, b') + (A - I_n)(x - x_a) \tag{3.1.2}$$

Every terms in the above equation are discussed briefly in the following section.

3.1.1 Retrieval noise

Retrieval noise is given by $G_y\epsilon$ and is usually the easiest component to evaluate. Measurement noise itself, ϵ, is usually random, generally unbiased and often uncorrelated between channels. It also has a known covariance matrix. The covariance of the retrieval noise is

$$S_m = G_yS_yG_y^T \tag{3.1.3}$$

3.1.2 Forward model error

This error source is defined as $G_yf = G_y[f(x, b, b') - F(x, b)]$. Modelling error can be difficult to evaluate as it requires a model for f which includes all of the correct physics. If this is possible (which is rarely the case for atmospheric physics due to the complex nature of the processes in the atmosphere) and the physics can be modelled accurately, and F is simply a numerical approximation then evaluating model error is straightforward. The forward model error source is likely to be systematic, which are due to uncertainties in instrument characterization and in input parameters of the radiative transfer, as well as to approximations in the forward model itself [12, 26].

3.1.3 Smoothing error

This error term arises when it is assumed that the retrieval is an estimate of the true state rather than an estimate of the state that has been smoothed by the averaging kernel. The true state will not be known in general (which is why the measurement is being made in the first place) thus the actual smoothing error cannot be estimated. Instead, the statistics of the error can be investigated from looking at the mean and covariance from an ensemble of states. To estimate the smoothing error covariance, the covariance matrix of a real ensemble of states must be known. The covariance matrix of smoothing error is expressed as

$$N = (A - I)S_a(A - I)^T \tag{3.1.4}$$

where I is the identity matrix and A is average kernel matrix which is obtained from the product of K_x and G_y.

3.1.4 Forward model parameter error

The error in the retrieval due to forward model parameter errors is $G_y K_b(b - b_a)$ which is caused by uncertainties in model parameters such as spectroscopic parameters, particularly, spectral line strength and line width parameters have been used in this work. Evaluation of G_y and K_b can be performed by perturbation from the inverse method and forward model respectively. If the forward model parameters have been estimated properly and assuming that the model is linear as far as they are concerned then their individual errors will be unbiased and the expected error will be zero. The covariance matrix of forward model parameter error is expressed as

$$P = (G_y K_b)S_b(G_y K_b)^T \tag{3.1.5}$$

If one knows the statistics of the spectroscopic parameters b, that means the covariance matrix of S_b is known, then the model error covariance matrix P, describing the resulting error on the retrieval, can be easily calculated using equation(3.1.5).

3.2 Gases considered for the sensitivity study

Water vapor (H_2O)

Atmospheric H_2O plays an important part in the troposphere in most phenomena associated with the "weather". It is the main component of the so-called green house gas. In the stratosphere, water vapor provides the primary source of the hydroxyl radial.

Methane (CH_4)

Methane has natural as well as anthropogenic source at the earth surface and diffuses into the stratosphere where it may affect the ozone cycle by acting as a source of odd hydrogen a sink of atomic chlorine. The troposphere concentration of CH_4 increases at a rate of 1% per year.

Nitrous oxide (N_2O)

Nitrous oxide is commonly known as laughing gas. A molecule of nitrous oxide is 200 to 300 times more effective than the molecule of carbon dioxide in the green house warming it produces. Its atmospheric life time is about 150 years. Nitrous oxide provides the primary source of stratospheric odd nitrogen (NO_y) by its reaction O('D). The stratospheric N_yO distribution is strongly controlled by atmospheric transport.

Nitric Acid (HNO_3)

Nitric acid plays an important role in the chemistry of the stratosphere because it is a reservoir for the odd nitrogen species which catalytically control the ozone abundance and it may act as a sink of stratospheric NO_y.

Ozone (O_3)

Ozone is the only atmospheric constituent which effectively absorbs ultraviolet solar

radiation from about 250 to 310nm, protecting plant and animal life from exposure to harmful radiation. The nineteen percent of ozone in the earth's atmosphere is in the stratosphere [28]. Ozone is produced in the upper atmosphere by incoming ultraviolet radiation causes oxygen molecules (O_2) to go to O+O. Some of them recombine with O_2 to make O_3. This ozone then absorbs more ultraviolet radiation and breaks down to O_2 to O. This O can then recombine with O_2 to make more ozone. This process is self regulating and results in less ultraviolet radiation reaching the earth's surface [29].

Sulfur dioxide (SO_2)

Sulfur dioxide is an important trace specie in the atmosphere, under background condition and in polluted area. It is related to the troposphere as a result of both anthropogenic and natural phenomena. Sulfur dioxide emission are partly responsible for acid depositions on the surface and the occurrence of winter smog episodes. In addition, the oxidation of SO_2 in the troposphere leading to concentration of sulfate aerosols in the atmosphere has also been found to contribute to visibility degradation. Volcanoes are an important natural source of various atmospheric trace gases. The main anthropogenic source of sulfur dioxide include fossil fuel consumption, the smelting of metal sulfide ore to obtain the pure metal and coal burning. In the dry stratosphere, particularly in the lower stratosphere where the concentration of OH is relatively small, the life time of SO_2 is longer than in the troposphere (of the order of several weeks) [30].

Microwindow (cm^{-1})	Trace gas	Interfering gases
2481.3000 - 2482.6000 2526.4000 - 2528.2000	N_2O	CO_2, H_2O, CH_4, O_3
2613.7000 - 2615.4000 2650.6000 - 2651.3000	CH_4	H_2O, CO_2, O_3, HDO, HCl,
2941.6000 - 2941.9000 2974.2000 - 2975.6000 2983.2000 - 2985.2000	H_2O	O_3, CH_4, HCl, C_2H_6, HDO
867.0000 - 868.5920 872.0000 - 872.6000	HNO_3	H_2O, CO_2
1000.0000 - 1002.0000 1020.4400 - 1020.8200 1022.5300 - 1022.9700	O_3	H_2O, N_2O, CH_4, CO_2, C_2H_6
1142.5200 - 1143.4000 1146.5800 - 1147.4000	SO_2	O_3, N_2O, H_2O, CH_4, HDO

Table 3.1: Microwindows listed in the table for gases considered in sensitivity studies

Chapter 4

Result and discussions

In this work, we have studied different atmospheric trace gases to assess the impact of uncertainties of spectroscopic parameters, particularly, those of spectral line strength and line width parameters on the retrieved VMR of the species. VMR of the target trace gases has been retrieved with actual spectroscopic parameters and perturbed spectroscopic parameters. Retrieval simulations are carried out for spectroscopic database containing the best available information on the spectroscopic parameters, as archived in HITRAN database.

Fig 4.1 shows the volume mixing ratio (VMR) profile of the targeted trace gases used in this study. The profiles help us to identify where the species are largely available. Based on this fact, our discussion of retrieval error due to uncertainty of spectroscopic parameters focus mainly on the altitude range where the species are largely abundant.

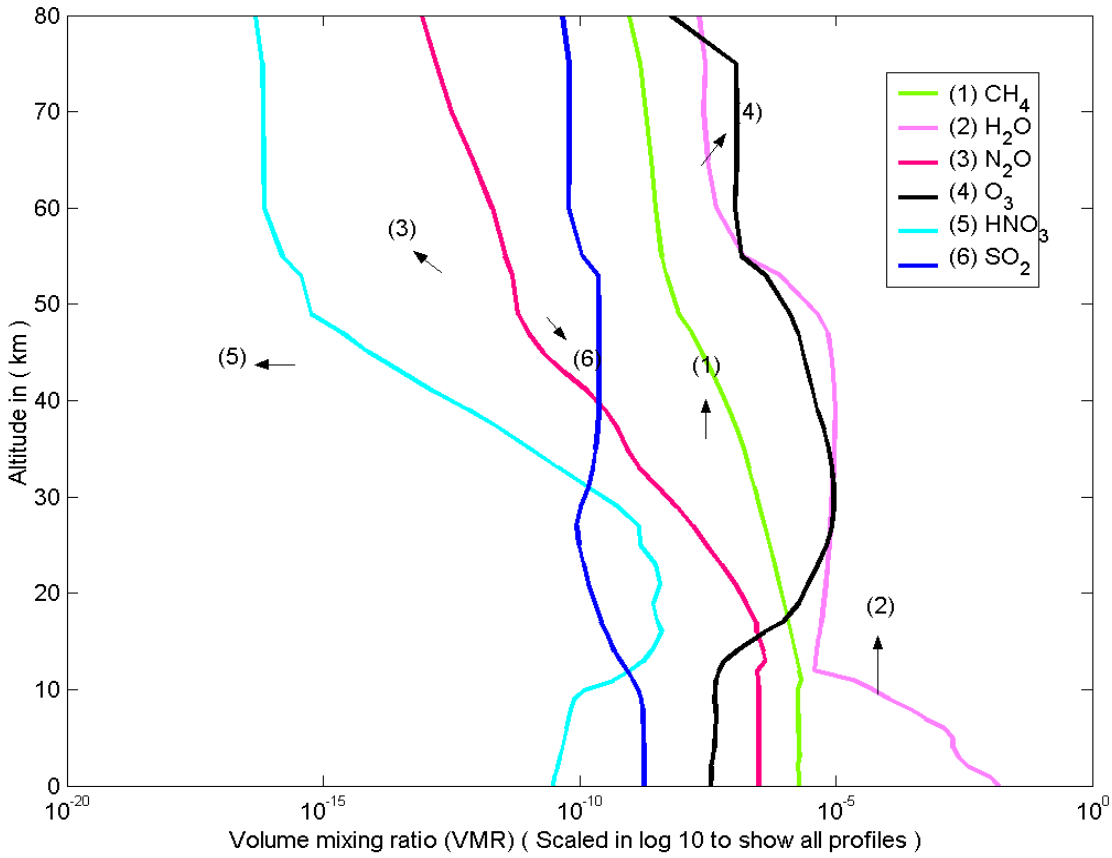

Figure 4.1: Concentration profiles of targeted atmospheric trace gases

4.1 Assessment of impact of spectral line strength on VMR

The retrieval simulations show that uncertainty of spectral line strength parameter is more visible at the strong signature of the species.

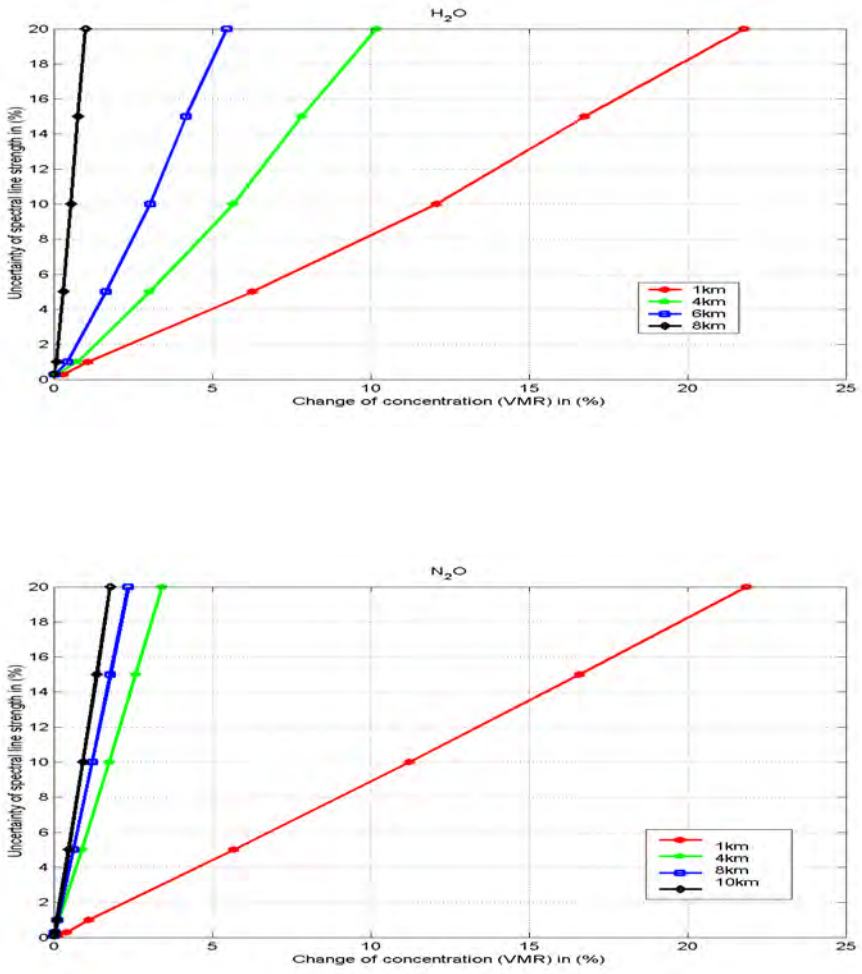

Figure 4.2: Uncertainty of spectral line strength versus error in the concentration of N_2O and H_2O at different altitudes.

Figs. 4.2, 4.3, 4.4, and 4.5 show the response in VMR to uncertainties in spectral

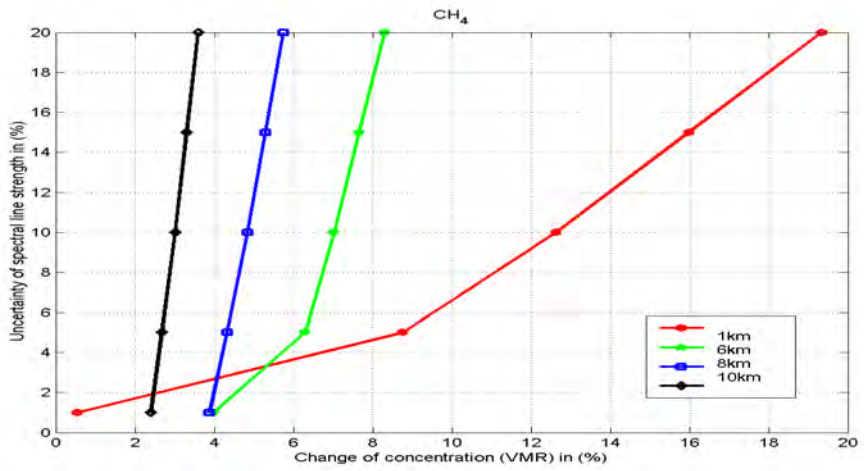

Figure 4.3: Uncertainty of spectral line strength versus error in the concentration of CH_4 at different altitudes.

line strength of H_2O, N_2O, HNO_3, O_3 and SO_2 respectively. Spectral line strength depends on the ground state population of molecular transitions. The ground state population is governed by Boltzman distribution. Therefore, it is natural to expect that ground state is highly populated when the VMR of a given trace gas is abundant. This relation is clearly exhibited by patterns observed in all figures (Figs 4.1, 4.2, and 4.3), though, the response is not direct at all altitude levels shown.

From Fig 4.2 (top panel) depicts, at the altitude of 1km there is almost linear relationship between change in the concentration of H_2O and uncertainties of spectral line strength. More specifically, at 1%, 5%, 10%, 15%, and 20% uncertainties of this parameter, we found the corresponding changes in the concentration to be 1.2%, 6.2%, 13%, 17%, and 23% respectively. On the other hand, at altitudes of 4 km, 6 km, and 8 km, the changes in concentration have shown appreciably successive decline respectively. In the same figure at bottom panel, change in the retrieved VMR of nitrous oxide (N_2O)is linear with the uncertainty of spectral line strength at the

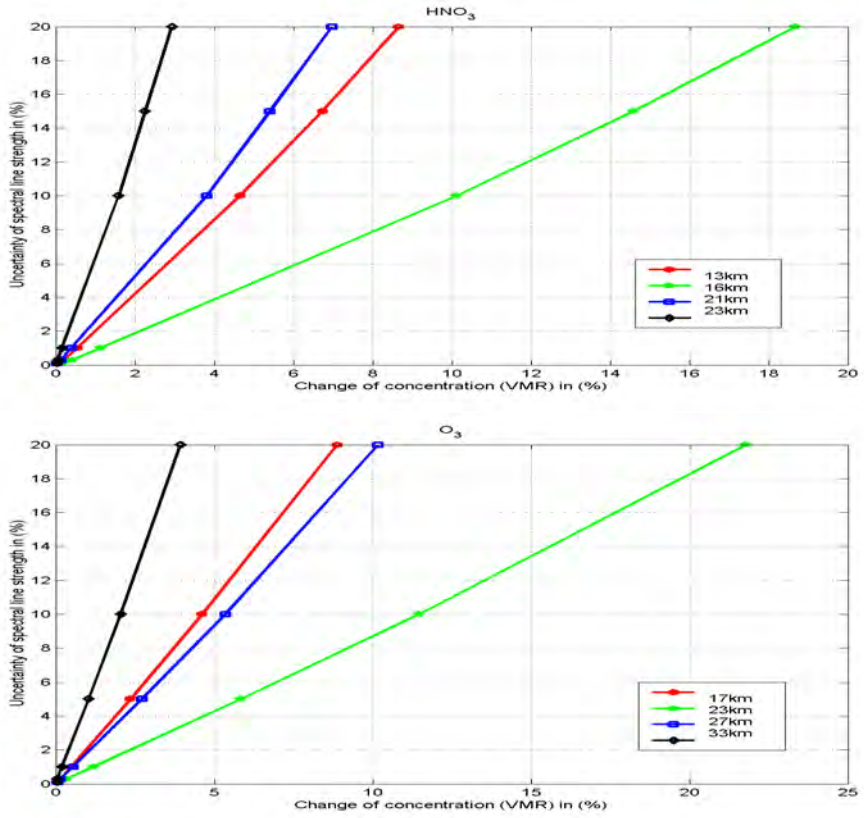

Figure 4.4: Uncertainty of spectral line strength versus error in the concentration of HNO_3 and O_3 at different altitudes.

same altitude of 1km even if there is a slight variation from H_2O. But other altitude (4 km, 8 km, 10 km), the response of the concentration to changes in the line strength has decreased successively with altitude.

The retrieval of methane (CH_4) VMR with perturbed and unperturbed spectral line strength have revealed similar response as in the case of H_2O and N_2O. The dominant and clearly linear changes is observed for the lowest altitudes. This is linked to the fact that all the three gases considered so far are source gases whose maxima are close to the land surface. This is obviously linked to the steep decline in CH_4 VMR as compared to that of N_2O for instance.

In the case of HNO_3 retrieval, we have got a comparable and linear change of magnitude in VMR with the value of uncertainty of parameter at 16 km (see top panel of figure 4.4). Above and below this altitude, the rate of changes in concentration decrement seem to be symmetrical in both parts. Similarly, the retrieval error of O_3 reaches a value of 22% at altitude of 23 km (see bottom panel of figure 4.4) corresponding to a 20% change in spectral line strength, which is a bit higher than (but almost linear with) the uncertainty of parameter.

More often, the retrieval of SO_2 concentration has been implemented by using scattering of radiation due to this species [27]. But, in this work, the retrieval was made based on absorbance because SO_2 is an infrared absorber. However, SO_2 signal is found in a spectral region where strong absorbers such as H_2O, O_3, N_2O are also found. The interferences from these trace gases make the retrieval of SO_2 a difficult task under normal atmospheric conditions. Optimal set of spectral grid points have been selected for retrieval of SO_2 on the basis of minimizing interferences from other gases. This microwindow selection (optimal set of spectral grid points) does not completely avoid interferences from other gases. With this limitation, the spectral line

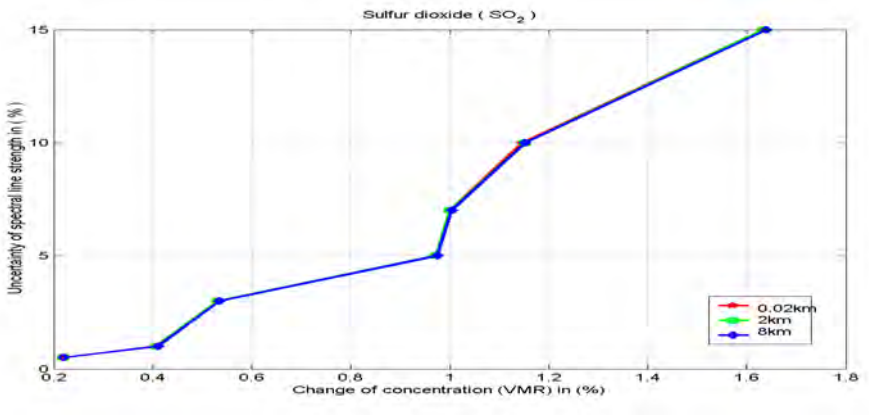

Figure 4.5: Uncertainty of spectral line strength versus error in the concentration of SO_2 at different altitudes.

strength has been perturbed in the range between 0.5% to 15%, which induced an error on the VMR in the interval between 0.21% to 1.62% (see Fig 4.5). Therefore, we have found that spectral line strength is not a major factor that determines accuracy of retrieved SO_2 VMR under normal atmospheric conditions.

4.2 Assessment of impact of pressure broadened halfwidth parameter

Line width is a spectroscopic parameter which includes pressure broadening halfwidth and self broadening halfwidth. The impact of pressure broadening halfwidth uncertainty has been assessed for H_2O, N_2O, O_3, HNO_3 and S_2O trace gases.

In the H_2O retrieval with perturbation of this parameter, noticeable changes on VMR at 2 km, whose magnitudes almost 10 times higher than the values of uncertainty, particularly, in the range between 0.2% to 0.5% have been observed. Moreover, the impact still remain strong at 5 km (see Fig 4.6). Considering N_2O, the magnified impact is dominated at 0.02 km where we have noticed that the change in VMR is

slightly less than the corresponding uncertainty.

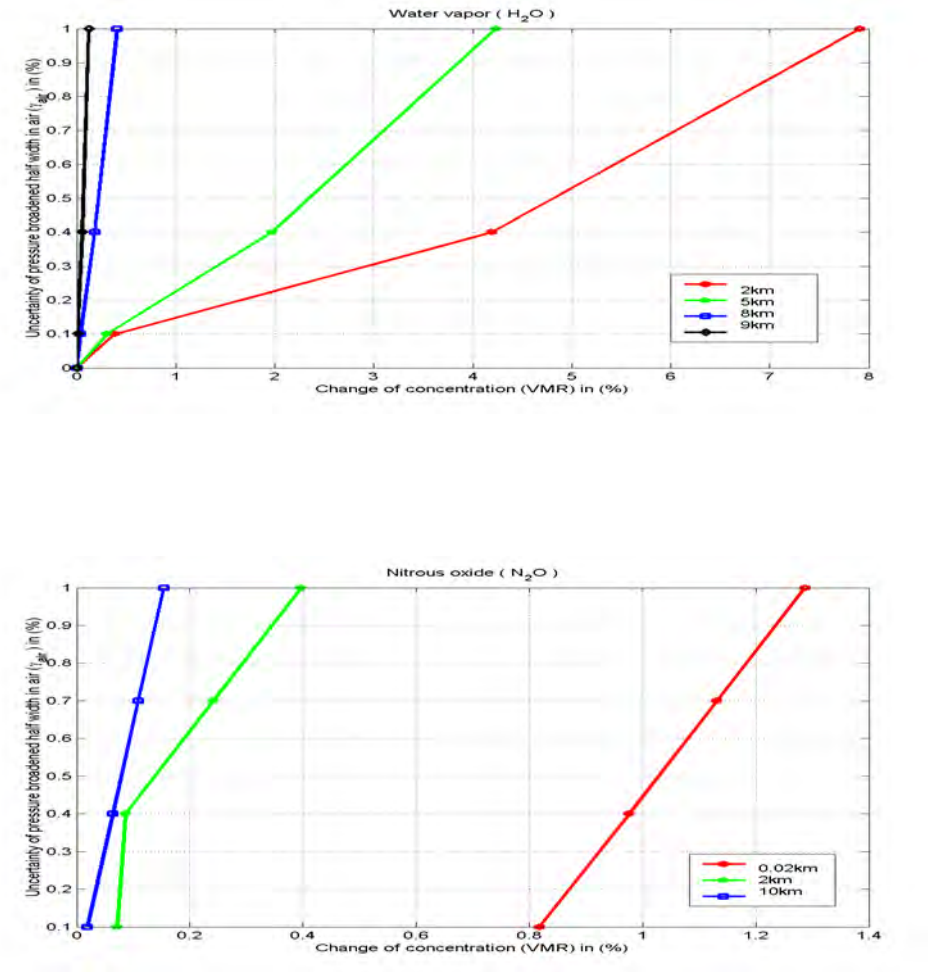

Figure 4.6: Uncertainty of pressure broadened halfwidth in air γ_{air} versus error in the concentration of H_2O and N_2O at different altitudes.

As can be seen from Fig 4.7 at the top panel, the investigated impact of this parameter on the concentration of HNO_3 is significant at the altitude of 17 km in the order of 1.1%. In the other parts of profile, the effect has been rather samll. When we look at the retrieval error of O_3 (see Fig 4.7 bottom panel), the impact is strong at 23

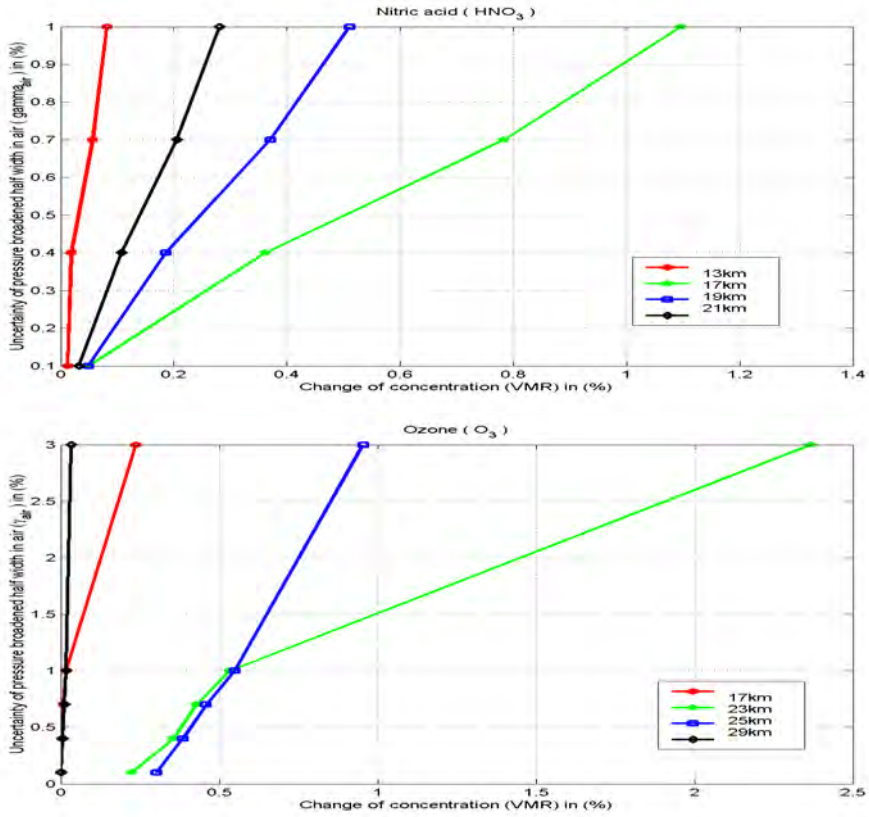

Figure 4.7: Uncertainty of pressure broadened halfwidth in air γ_{air} versus error in the concentration of HNO_3 and O_3 at different altitudes.

km where the perturbed value was taken up to 3%, which generates an error of 2.4% comparable value as that of the half line width.

We have described why the retrieval SO_2 gas concentration is difficult under normal atmospheric condition in the above section. The perturbation of pressure broadened halfwidth was made in the range between 0.1% to 3%, which attributes the change in VMR of SO_2 gas in the interval between 0.23% to 0.65% (see Fig 4.8). The impact of this parameter on the VMR change is relatively weak as its uncertainty increases.

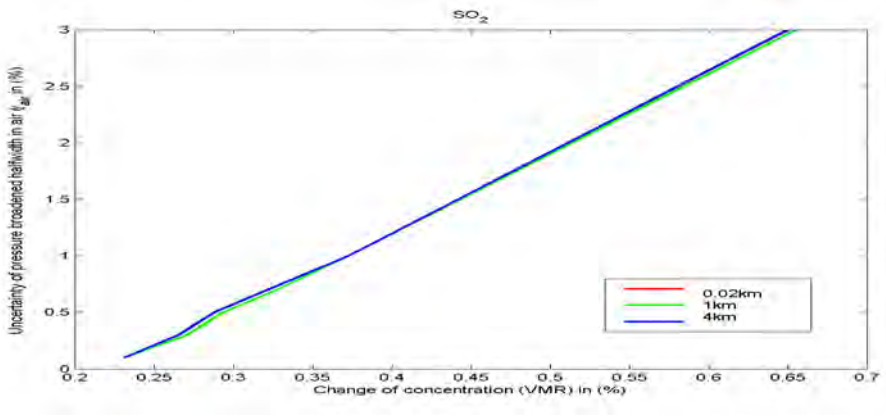

Figure 4.8: Uncertainty of pressure broadened halfwidth in air γ_{air} versus error in the concentration of SO_2 at different altitudes.

4.3 Investigation on the relationship of simulated part of forward model with retrieved state vectors

The forward model provides a physical description of the measurement process and a numerical simulation of radiative transfer which are used for retrieval of atmospheric state such as concentration profile. In this part of discussion, the main focus is to investigate the linearity of the forward model with respect to resulting change in concentration due to uncertainties in spectroscopic parameters. Fig 4.9 and Fig 4.10 show the change in simulated part and VMR due to uncertainties of spectral line strength of N_2O and CH_4. Uncertainty of spectral line strength induced a change in simulated part because they have direct relationship according to radiative transfer equation. In order to show whether the change in simulated part with the change in VMR of the species linear or not, we have used our assumption of $\delta_F = K_x\delta_x$. To obtain the change in concentration and the change in simulated spectrum, the

perturbation of spectroscopic parameter was made for 1%, 5%, 10%, 15% and 20%, for which spectral line strength parameter has been accounted. As a result, the product of Jacobian matrix with concentration difference ($K_x\delta_x$) and the change of simulated spectrum (δ_F) have been increased.

To illustrate more (see figure 4.9), 10%, and 20% uncertainty of this parameter attributed to the change in simulated spectrum at a maximum of 9.5×10^{-3}, 17×10^{-3} respectively. Similarly, $K_x\delta_x$ also increased but the order is much less than 10^6 with that of perturbation. The relation exhibited by the patterns observed in figure cited is not linear. So, in order to satisfy our assumption, there should be some higher order terms included (see section 2.2.3 for better discussion).

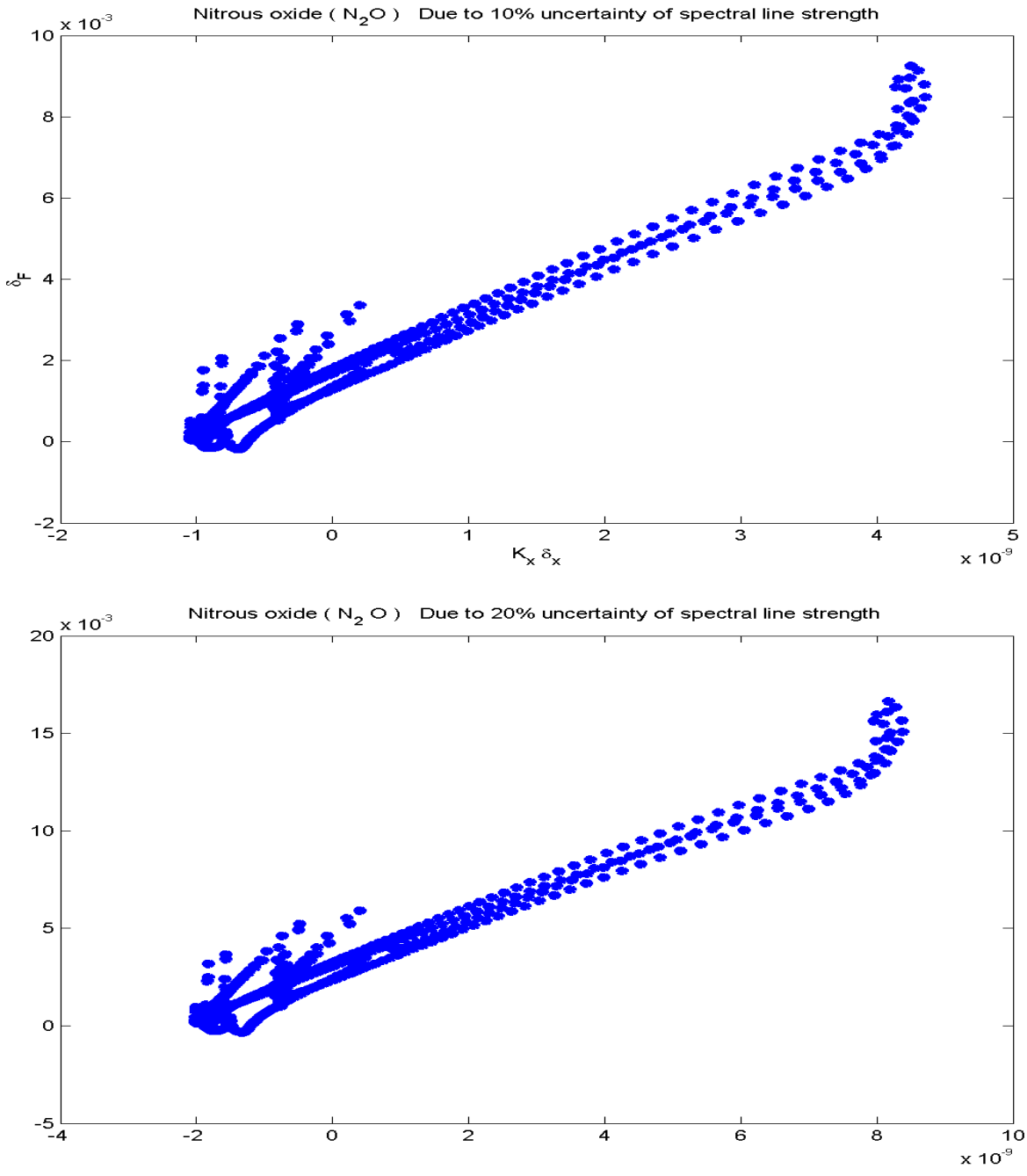

Figure 4.9: The change of transmitted spectrum versus the product of Jacobian matrix with concentration difference of N_2O gas.

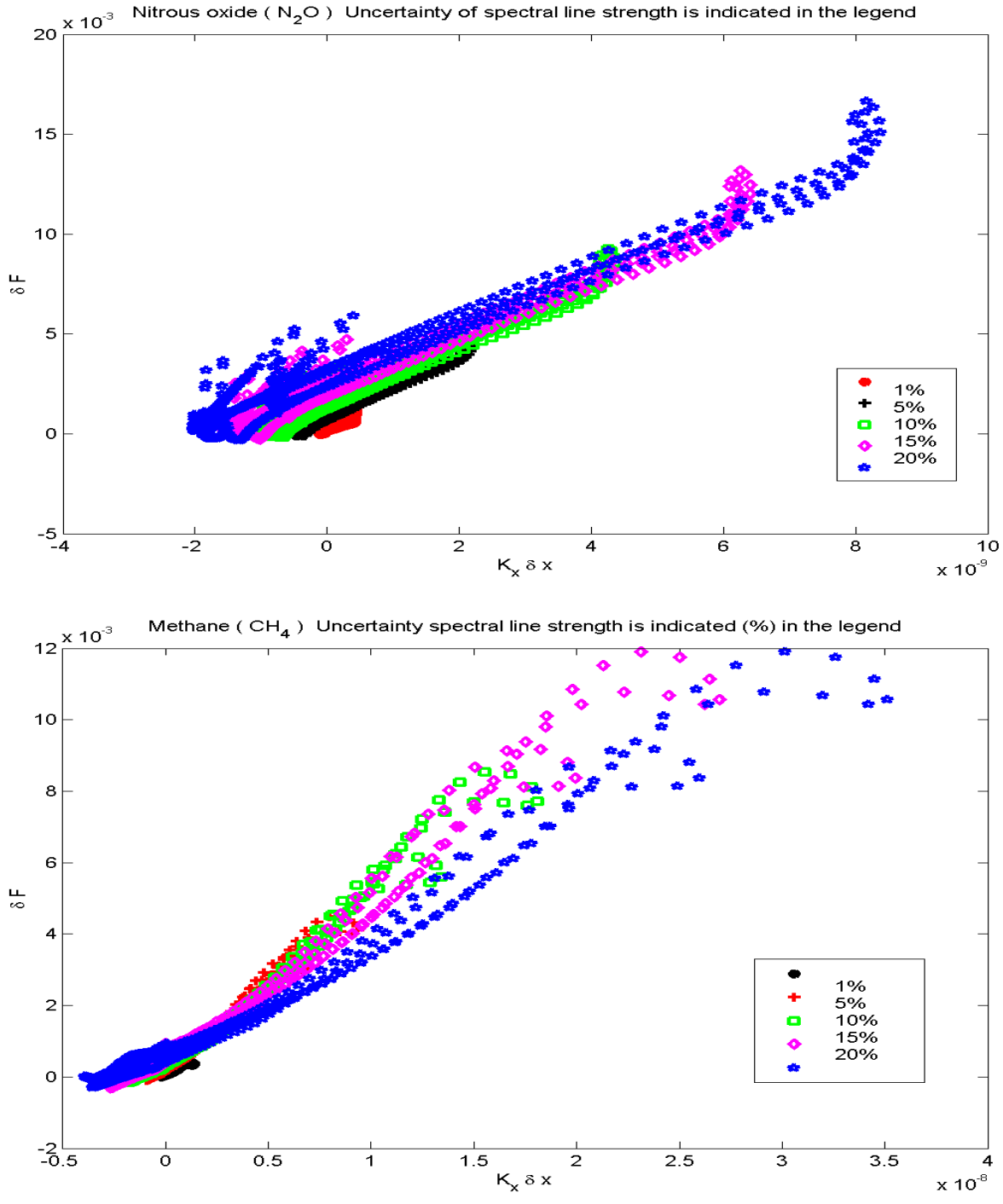

Figure 4.10: The change of transmitted spectrum versus the product of Jacobian matrix with concentration difference of N_2O and CH_4 gases.

Chapter 5

Conclusion

In this work, we have described different basic concepts such as spectroscopic parameters, radiative transfer, retrieval theory and error analysis. In order to assess the sensitivity of the retrieved state vector to spectroscopic parameters, the retrieval simulation is necessary. For this investigation, we have selected atmospheric trace gases, namely, water vapor (H_2O), ozone (O_3), methane (CH_4), nitrous oxide (N_2O), nitric Acid (HNO_3), and sulfur dioxide (SO_2).

Retrieval theory needs a direct measurement in order to derive the required atmospheric parameters. The retrieval simulation has been done based on optimal estimation which describes the relationship between the remote measurements and the true atmospheric state, with thorough error analysis involved. Different types of errors in the retrieval process have been identified. Namely retrieval noise, smoothing error, forward model error, and forward model parameters error. In this part of work, we have dealt with uncertainty of spectroscopic parameters, which are included in the source of forward model parameters error. The study has focused on spectral line strength and pressure broadened halfwidth coefficient. Uncertainty of pressure broadened halfwidth has led to a retrieval error, whose effect is more effectively observed at the strong lines of the targeted species. When studying the impact of this parameter

in those targeted trace gases such as H_2O, N_2O, O_3, and HNO_3, the magnitude of retrieval error is relatively high at the peak value of VMR. More specifically, error caused by this parameter is so strong in H_2O gas as compared to other trace gases. In a similar manner, the perturbation of spectral line strength has caused a significant error in the retrieval of the species concerned. In H_2O, N_2O, and CH_4 gases, the maximum error has been recorded around the surface. In the case of HNO_3 and O_3, the strong impact has been resulted in around 16 km and 23 km respectively. As a result, those parameters will have a significant impact on the accuracy of atmospheric trace gases abundance.

Bibliography

[1] Rinsland C.P., et.al., Northern and Sourthen hemisphere ground based infrared spectroscopic measurements of tropospheric gas Carbon Monoxide and Ethane, J Geophy. Res, 103, 28197 - 28218, 1998.

[2] Drusch M., Crewell S, Principle of radiative transfer, European center for medium-range weather forcasts, reading, UK Munich university, Germany, 2005.

[3] Moore D.P,Waterfall A..M, Remedios J.J, The potential for radiometeric retrievals of halocarbon concentration from the MIPAS-E instrument, Earth observation science, department of physics and Astronomy, university of leicester, 2006.

[4] Rothman, L.S. et.al., The HITRAN Molecular Spectroscopic Database and HAWKS (HITRAN Atmospheric Workstation): 1996 Edition, J. Quant. Spectrosc. Radiat. Transfer, 60, 665-710, 1998.

[5] Verdes C.L et. al., A sensitivity study on spectroscopic parameter accuracies for a mm/submm limb sounder instrument, Journal of molecular spectroscopic 229, p266-275, 2005.

[6] Verdes C.L, A.Von Englena, S.A. Buehlera, A.Perrinb, partition function data and impact on retrieval quality for an mm/sub-mm limb sounder, Journal of spec. and Radiative Transfer p1-21, 2004.

[7] Andrei T. , Introductory Quantum mechanics II, MIT department of chemistry, 2005.

[8] Stefan A. Buhler, Remote sensing of atmospheric composition for climate applications, atmospheric department, Bremen university, Germany, 2004.

[9] Erwan M. , Retrieval characterization of a double sideband radiometer for simultaneous observation of ozone and carbon monoxide, department of radio and space science, chalmers university of technology Goteborg, Sweden, 2004.

[10] Orphal J., High resolution molecular spectroscopy for atmospheric studies, laboratory for photophysique molecular C.N.R.S, University of Orsay, France, 2001.

[11] Irikura karl K. , Essential statistical thermodynamics, physical and chemical properties division, National Institute of standards and Technology, Gaithersburg, MD 20899, 1998.

[12] David M. Philip, measurement of HCFC-22 in the upper troposphere and lower stratosphere from the MIPAS-E instrument, PhD thesis, at the universisty of leicester, 2005.

[13] Mengistu G. Determination optimized microwindows for analysis of absorption spectra from ground-based FTIR spectrometers, MSc. thesis, 1998.

[14] Liou, K.N., An introduction to Atmospheric radiation, Acadamic Press. Inc, 1980.

[15] Chandrasekhar, S., Radiative Transfer, Dover publications, Inc., New York, 1960.

[16] Yakub A. Tijani, multi-annual study of chlorine species in the stratosphere using airborne microwave measurements, Msc. thesis, Institute of environmental physics, university of Bremen, Germany, 2004.

[17] Pan et al., Satellite remote sensing of troposperic CO and CH4; forward model studies of MOPITT instrument, 1995.

[18] Melsheimer C., Verdes C., et.al., Intercomparison of general purpose clear sky atmospheric radiative transfer models for the millimeter/submillimeter spectral range, Radio Science, Vol.40, RS1007, 2005.

[19] C. Clerbaux, et.al., Trace gas measurements from infrared satellite for chemistry and climate applications, c Atmos. Chem. Phys. Discuss., 3, 2027 - 2058, 2003

[20] Frankenberg C, Platt U, and Wagner T., Iterative maximum a posteriori (IMAP)-DOAS for retrieval of strongly absorbing trace gases: Model studies for CH4 and CO2 retrieval from near infrared spectra of SCIAMACHY onboard ENVISAT, Atmos. Chem. Phys., 5, 9 -22, 2005.

[21] Daniel J. Jacob, lectures on inverse modeling, Harvard university, 2007.

[22] Vigouroux C., De Maziere M., et.al., Comparisons between ground-based FTIR and MIPAS N_2O and HNO_3 profiles before and after assimilation in BASCOE, Atmos. Chem. Phys., 7, 377396, 2007.

[23] Raspollini P., et al., MIPAS level 2 operational analysis, Atmos. Chem. Phy. Discuss.,6, 6525-6585, 2006.

[24] Shepard A. Clough, Mark W.Shephard, et.al., Forward Model and Jacobians for Tropospheric Emission Spectrometer Retrievals, IEEE Transactions on Geoscience and Remote Sensing, VOL. 44, NO. 5, MAY 2006.

[25] Kagawa A., et al., Characterstics and error estimations of stratospheric ozone and ozone-related species over Poker Flat (65^oN, 147^oW), Alaska observed by ground based FTIR spectrometer from 2001 to 2003, Atmos. Chem. Discuss.,6, p10299 to 10339, 2006.

[26] Hendrick F., et al., Retrieval of nitrogen dioxide stratospheric profiles from ground-based zenith-sky UV-visible observations: validation of the technique through correlative comparisons, Atmos. Chem. Phys. Discuss., 4, 28672904, 2004.

[27] W. Thomas W., et al., Retrieval of volcanic sulfur dixide emission from GOME backscatter measurements, Deutscher Wetterdienst (DWD), Dept. Climate and Environment, P.O. Box 10 04 65, D-63004 Offenbach, Germany, 2005.

[28] Echle G., H.Oelhaf, A.Wegner, Measurement of atmospheric parameter with MIPAS final report, ESA contract 9597/91/NI/SF, December 1992.

[29] Uherek E., Formation of ozone, Max Planck Institute for Chemistry, Mainz, Germany, 2004.

[30] Burgess A.B., Grainger R.G., Dudhia A., progress in the retrieval sulfur species from MIPS, Atmospheric, Oceanic and Planetary Physics, Department of Physics, University of Oxford, 2004.

Declaration

I hereby declare that this thesis is my original work and has not been presented for a degree in any other university. All sources of material used for the thesis have been duly acknowledged.

Name: Samuel Takele

Signature: .....

This thesis has been submitted for the examination with my approval as university advisor.

Name: Dr. Gizaw Mengistu

Signature: .....

Addis Ababa University
Department of Physics
July, 2007